Published in final edited form as:
Cancer Res. 2015 August 1; 75(15): 3098–3107. doi:10.1158/0008-5472.CAN-15-1227.

Interleukin-6 stimulates defective angiogenesis

Ganga Gopinathan[1], **Carla Milagre**[1], **Oliver M.T. Pearce**[1], **Louise E. Reynolds**[1], **Kairbaan Hodivala-Dilke**[1], **David A. Leinster**[1], **Haihong Zhong**[2], **Robert E. Hollingsworth**[2], **Richard Thompson**[1], **James R. Whiteford**[3], and **Frances Balkwill**[1]

[1]Barts Cancer Institute, Queen Mary University of London, Charterhouse Square, London EC1M 6BQ UK

[2]MedImmune, One MedImmune Way, Gaithersburg, MD 20878 USA

[3]William Harvey Institute, Queen Mary University of London, Charterhouse Square, London EC1M 6BQ UK

Abstract

The cytokine interleukin-6 (IL-6) has a number of tumor-promoting activities in human and experimental cancers, but its potential as an angiogenic agent has not been fully investigated. Here we show that IL-6 can directly induce vessel sprouting in the *ex vivo* aortic ring model, as well as endothelial cell proliferation and migration, with similar potency to VEGF. However, IL-6-stimulated aortic ring vessel sprouts had defective pericyte coverage compared to VEGF-stimulated vessels. The mechanism of IL-6 action on pericytes involved stimulation of the Notch ligand Jagged1 as well as Angiopoietin2 (Ang2). When peritoneal xenografts of ovarian cancer were treated with an anti-IL-6 antibody, pericyte coverage of vessels was restored. In addition, in human ovarian cancer biopsies there was an association between levels of IL-6mRNA, Jagged1 and Ang2. Our findings have implications for the use of cancer therapies that target VEGF or IL-6 and for understanding abnormal angiogenesis in cancers, chronic inflammatory disease and stroke.

Introduction

Interleukin-6, IL-6, is a major tumor-promoting cytokine produced by both malignant and host cells in the tumor microenvironment [1]. It is also a downstream product of oncogenic mutations, *e.g.*, ras and TP53 [23]. Typically via its major downstream signal transducer STAT3, IL-6 has both local and systemic pro-tumor actions in experimental and human cancers. In the tumor microenvironment, these include stimulation of malignant cell growth and survival [4], promotion of invasion and metastasis [5], modulation of tumor-promoting T cell subtypes, involvement in autocrine tumor cell cytokine networks [6], and regulation of the

Author Contributions

F.B, J.R.W, K.H-D and G.G designed the experiments. G.G carried out majority of the experimental work. C.S and R.H performed the animal experiments. O.M.T.P conducted the RNAseq analysis. L.E.R provided essential reagents and A.D.L helped with the set up of the aortic ring experiments. R.E.H and H.Z provided the anti-IL-6 antibody (MEDI5117), advised on its use and contributed to the manuscript. J.R.W helped with the migration assays. F.B and G.G wrote the manuscript. All authors reviewed the manuscript.

Disclosure of Potential Conflicts of Interest

Robert E. Hollingsworth is the senior director, oncology research in MedImmune. No potential conflicts of interest were disclosed by the other authors.

Europe PMC Funders Author Manuscripts

myeloid cell infiltrate [7]. Systemic effects of excess IL-6 production include induction of acute phase reactants and involvement in the elevated platelet count (paraneoplastic thrombocytosis) [8] that is a complication of several common human cancers.

To add to this catalogue of tumor-promoting actions, there are reports that IL-6 stimulates angiogenesis in the tumor microenvironment [9] with evidence that STAT3 signaling induces HIF-1 mediated VEGF-A transcription [10]. IL-6 is also reported to have direct effects on endothelial cell proliferation and migration [91112] and has been implicated in resistance to anti-VEGF antibody treatment in patients [1314]. In preclinical and clinical studies we found that a therapeutic neutralizing anti-IL-6 antibody reduced systemic VEGF levels in ovarian cancer patients, and that in peritoneal ovarian cancer xenografts, blood vessels were reduced, with a concomitant inhibition of the Notch ligand Jagged 1 [7].

This led us to study further the actions of IL-6 in normal and cancer angiogenesis. In this paper we present novel evidence that IL-6 directly stimulates angiogenesis, but in contrast to VEGF, IL-6 stimulated vessels have defective pericyte coverage. We show that this may be due to differential regulation of Notch ligands and Ang2 by these two mediators. Our findings have implications for the use of cancer therapies that target VEGF or IL-6.

Methods

Ethics Statement

All animal experiments were approved by the local ethics review process of the Biological Services Unit, Queen Mary University of London and conducted in accordance with the UKCCCR guidelines for the welfare and use of animals in cancer research.

Aortic ring assay

Angiogenic sprouts were induced from mouse or rat thoracic aortas according to the method of Nicosia and Ottinetti [40]. Aortas were dissected from cervically dislocated 8-12 week old male C57BL/6 mice (Charles River) or 180–200g male Wistar rats (Harlan Laboratories) and sliced into 0.5 mm sections and incubated overnight in serum free OptiMEM (Invitrogen) at 37°C. Aortic rings were embedded in type I collagen (1 mg/ml) in E4 media (Invitrogen). For mouse aortic rings, the wells were supplemented with OptiMEM with 1% FBS and 30ng/ml of VEGF (R&D systems), 50ng/ml of human IL-6 (R&D systems) or 30ng/ml of mouse IL-6 (R&D systems) and incubated at 37°C, 10% CO_2. Rat aortic ring wells were treated with OptiMEM with 1% FBS and 10ng/ml VEGF, 10ng/ml rat IL-6 or 10nM VEGFRi (Cediranib, VEGFR2 inhibitor) and incubated at 37°C, 10% CO_2. Angiogenic sprouts were counted after 7 days of culture for mouse aortic ring and after 4 days of culture for rat aortic rings. The length of sprouts was quantified using ImageJ software by drawing radial lines from the base of the aortic ring to the tip of the sprouting new vessel. Pericytes were quantified 250 microns from the tip of the aortic ring vessel to avoid false positive quantification of activated fibroblast, which are normally found at the stalk of the vessel. Animals were housed and treated in Accordance with UK Home Office Regulations.

Staining of Aortic rings

The rat and mouse aortic rings were respectively cultured for 1 and 2 weeks before the staining. The rings were washed with PBS, fixed in 4% formaldehyde for 20 minutes. The wells were then washed once in PBS and the rings were permeabilized with 0.5% Triton X-100 in PBS for 30 minutes, before being washed twice in PBS. 100μl of BS-1 Lectin FITC (1 mg/ml; Sigma, cat. no. L9381/L5264) (1:200), anti-actin, α-SMA Cy3 (Sigma, cat. no. C6198) (1:500) or anti-NG2 (Millipore, ab5320) (1:200) was added and incubated overnight at 4°C. For IL-6Rα staining on aortic rings, 100μl of the unconjugated (1:200) IL-6Rα antibody was left overnight at 4°C. The following day the rings were washed with PBS and incubated with goat anti-rabbit Alexa 488 antibody (Life Technologies, A-11034) for 2 hours at room temperature. The plates were washed twice in PBS and the rings were removed from the 96 well plate, using a syringe needle, placed on a microscope slide and mounted with Prolong Gold DAPI containing medium (Invitrogen, cat. no. P36931). The slides were left to dry and imaged using confocal microscopy (Zeiss LSM 510 META).

Tissue culture

MLEC was kindly given by Professor Kairbaan Hodivala-Dilke, was used for most of the *in vitro* studies. This cell line was isolated and cultured as described previously [16]. HUVEC (HPA laboratories) were grown and cultured in endothelial growth medium (HPA laboratories) and maintained within 3-4 passages.

Ovarian cancer cell lines

The IGROV-1 line was recently characterized as a hypermutated line but unlikely to represent HGSC. The cell line was mycoplasma tested (InvivoGen, USA) and always maintained within 4-5 passages before new cells were recovered from frozen master stocks. Cells were cultured in RPMI 1640 supplemented with 10% FCS and 1% pen-strep. Cells were counted using a Vi-cell cell counter (Beckman Coulter) on days 3 and 7.

Staining of MLEC

2×10^5 MLEC cells were plated on a coverslip in a 12 well plate. The coverslips were fixed with 4% formaldehyde for 30 minutes and washed with PBS (3 times for 5 minutes each). Following fixation the cells were permeabilized with 0.1% Triton for 20 minutes and washed again in PBS. The cover slips were incubated with (1:200) rabbit IgG (R&D), (1:300) Endomucin antibody (Santa Cruz Sc-65495), IL-6Rα antibody (1:200) (Santa Cruz C-20, Sc-661) overnight at 4°C. The following day the cover slips were incubated with secondary (1:2000) goat anti-rabbit Alexa 488 (Life Technologies, A-11034) for 2 hours at room temperature and then mounted on slides with Prolong Gold DAPI containing medium (Invitrogen, P36931). The images were taken using confocal microscopy (Zeiss LSM 510 META).

Western Blotting

2×10^5 MLEC or HUVEC were plated in a 6 well plate with 2ml MLEC medium (10%FBS). The following day the supernatant was removed and the cells were treated with VEGF (30ng/ml), human IL-6 (30ng/ml) or mouse IL-6 (30ng/ml) in 2ml of serum free MLEC

medium for 6 hours or 24 hours. Cells were then washed with PBS and harvested using RIPA Buffer (R0278, Sigma UK) with 1× proteinase inhibitors. Protein quantification was performed using the Bradford reagent (Sigma-Aldrich), according to the manufacturer's instructions. Cell extracts (25 μg) were run on a NuPAGE® Novex® 4-12% Bis-Tris Gels, 1.5 mm and transferred to a nylon membrane. The membrane was blocked overnight (4°C in PBS with 0.1% Tween and 5% milk powder) and probed using the following antibodies: Jagged1 (1:1000, Abcam ab7771), DLL4 (1:1000, Abcam ab7280), Ang2 (1:500, Abcam ab8452), Hey1 (1:500, Abcam ab22614), Phospho-Stat3 (Tyr705) (1:1000, Cell Signaling 9145), Stat3 (1:1000, Cell Signaling 4904), p-ERK (1:1000, Santa Cruz sc-7383), ERK (1:1000, Cell Signaling 9102), β-Actin (1:5000, Sigma A5316/). A rabbit or mouse horseradish peroxidase-conjugated secondary antibody (GE Healthcare, Chalfont St Giles, UK) incubation allowed visualization using enhanced chemiluminescence (ECL) (GE Healthcare). Protein concentration equivalence was confirmed by anti-β-actin antibody.

Scratch wound migration assay

Confluent monolayers of MLEC cells were scratched with a p20 pipette tip, cells were then washed twice with PBS prior to the addition of serum free growth medium with VEGF 100ng/ml, hIL-6 100ng/ml and mIL-6 100ng/ml. Wounds were monitored by time lapse microscopy using an Olympus IX81 Microscope Hamamatsu Orca ER digital camera. Images were acquired every 30 minutes and subsequently analyzed using ImageJ software.

Cell proliferation assay

70,000 MLEC cells were seeded in a 24 well plate. The following day cells were treated with either 50 or 100ng/ml of VEGF, human IL-6 or mouse IL-6. The plate was then incubated for 72 hours at 37°C and 5% CO2. After incubation, the cells were trypsinized and counted using the Vi-cell counter (Beckman Coutler). Each condition was repeated in triplicate.

In vivo IGROV-1 xenografts

A total of 1×10^7 luciferase-expressing IGROV-1 cells (IGROV-1luc) were injected intraperitoneally (i.p.) into 20g 6 to 8 week-old female BALB/c nu/nu mice (purchased from Charles River, UK Ltd). After 24 hours, anti-IL-6 antibody (MEDI5117) was prepared at a concentration of 20mg/kg in sterile, endotoxin free, PBS and mice were injected i.p with 200μl of this solution twice weekly for 4 weeks. Control mice were injected with 200μl of 20mg/kg IgG control antibody. MEDI5117 is a human immunoglobulin G1 kappa (IgG1κ) monoclonal antibody that binds to interleukin 6 (IL-6) with sub-pM affinity and neutralizes it by preventing the binding to IL-6Rα. MEDI5117 was generated using phage display technology. It bears a triple mutation (referred to as YTE) in the Fc domain of the heavy chain that extends its half-life in circulation. MEDI5117 is active in several preclinical cancer models, including NSCLC, prostate cancer, breast cancer, and ovarian cancer (Zhong, H., *et. al.*, *Mol Cancer Ther*, in revision). An IgG1 isotype control antibody was generated by Medimmune and was used at the same concentration as MEDI5117. To visualize the architecture of blood vessels, some of the animals were anesthetized after 4 weeks of treatment and injected with FITC-conjugated *Lycopersicon esculentum* lectin

(tomato lectin; 100 μL, 2 mg/mL; Vector Laboratories) via the tail vein 3 minutes before animals were perfused with 4% paraformaldehyde under terminal anesthesia. Samples were processed and frozen sections were cut for Immunocytochemistry analysis for pericyte markers. The frozen sections from the lectin stained *in vivo* sections were permeabilized in 0.5% Triton X-100 for 30 minutes and washed 3 times in PBS. The sides were incubated overnight with 1:100 anti-α-SMA FITC (abcam, ab8211), 1:100 Mouse IgG2a (FITC) isotype control (ab81197), 1:50 or anti-NG2 (Millipore, ab5320) at 4°C. Primary antibody was washed with PBS. Slides were counterstained with DAPI Prolong Gold (Invitrogen) and images captured by confocal microscopy (Zeiss LSM S10 META).

Protein extraction from mouse tumors

75mg of tumor tissue was lysed with 1ml of ice-cold lysis buffer (150mM NaCl 20mM Tris, pH 7.5 1mM EDTA 1mM EGTA 1% Triton X-100) with protease and Phosphatase Inhibitors. Samples were then dissociated using gentleMACS Dissociator. After dissociation, samples were centrifuged at 1500 rpm for 2 minutes. Samples are always kept on ice between procedures. Next, using a probe sonicator set at 40% amplitude, tissues were sonicated for 5-15 seconds bursts. Sonicated samples were then rotated for 30 minutes at 4°C followed by a centrifugation for 15 minutes at 13,200 rpm at 4C. The pellet was discarded and protein concentration measured. Lysates were frozen at −80°C until loaded on gels.

Immunohistochemistry

Paraffin-embedded sections of tumor sections collected from IGROV-1 mouse xenograft were stained with antibodies for Jagged1 (1:100, R&D Systems, AF1277), DLL4 (1:100, R&D Systems, AF1389) Ang2 (1:50, Abcam, AB8452). Slides were counterstained with haematoxylin. Negative controls were isotype matched. The conditions used for staining with individual antibodies were in accord with manufacturers' recommendations.

Gene Expression Analysis

Table generated from a heat map established in a previous study (Coward et al).

Statistical analysis

Statistical analyses were carried out using Prism Graph Pad software. Statistical significance was calculated using Student's t test and chi-square test. Findings are presented as standard error of the mean (SEM).

Results

IL-6 stimulates angiogenesis in the aortic ring assay

As we had found that anti-human IL-6 reduced tumor blood vessel density in human tumor xenografts [7], we tested the activity of human IL-6 in the aortic ring assay. This is an *ex vivo model* of angiogenesis that studies the effects of mediators on normal vessel sprouting. Optimal vessel sprouting was observed in the mouse aortic ring assay 7-10 days after treatment with 30ng/ml VEGF or 50ng/ml hIL-6 (Figure 1A). Mouse IL-6 (30ng/ml) in

mouse aortas and rat IL-6 (10ng/ml) in rat aortas also stimulated vessel sprouting and there was no significant difference in the number of sprouts between the VEGF and IL-6 treatments (Figure 1B). VEGF and IL-6 treatments also gave similar results in terms of length of vessel sprouts (Figure 1C).

Other reports have described that IL-6 has indirect angiogenic activity via stimulation of VEGF production, and thus inhibition of VEGF action would also block IL-6 activity [15]. We therefore tested the action of the VEGF receptor inhibitor cediranib in the rat aortic ring assay. Cediranib significantly inhibited the sprouting activity of VEGF but had no significant activity on the actions of IL-6 in this model (Figure 1D). This result suggested that in the aortic ring model IL-6 may stimulate vessel sprout formation without inducing VEGF. To demonstrate that IL-6Rα is required for IL-6 mediated angiogenesis, we added an anti-IL-6Rα antibody to the IL-6 –simulated aortic ring cultures. This abolished the effect of IL-6 (data not shown). We also found that the endothelial cells of the aortic ring vessels expressed IL-6 receptor, staining positive for the gp80 IL-6 receptor alpha subunit (IL-6Rα) (Figure 1E). Furthermore western blots of lysates from the aortic ring assay showed strong induction of STAT3 phosphorylation by mouse IL-6 but only weak induction by VEGF (Figure 1F, Supplementary Figure 1). In contrast there was strong phosphorylation of ERK in VEGF-stimulated aortic ring lysates but IL-6 had no effect (Figure 1F, Supplementary Figure 1).

As the aortic ring assay has a mixture of cells that could complicate any analysis of signaling pathways, we used a simpler experimental system in our next set of experiments, the MLEC mouse endothelial cell line [16].

IL-6 has direct effects on endothelial cells

Mouse lung endothelial cells (MLEC) stained with the endothelial cell marker endomucin express IL-6Rα (Figure 2A), and both human and mouse IL-6 at 100 ng/ml stimulated MLEC proliferation (Figure 2B). The IL-6 effect was not as potent as that of VEGF but was still significant. VEGF and human and mouse IL-6 were equally potent in the ‘scratch’ assay which measured MLEC migration (Figure 2C). We then used western blotting to study the VEGF and IL-6 signaling pathways in these cells. As expected, IL-6 increased STAT3 phosphorylation and VEGF increased ERK phosphorylation, but IL-6 stimulation did not affect phospho-ERK levels and VEGF had no effect on phospho-STAT3 (Figure 2D, Supplementary Figure 2) after 24 hours of treatment. Similar results were observed in human umbilical vein endothelial cells (HUVEC) after treatment with human IL-6 (hIL-6) or VEGF (Supplementary Figure 3). Earlier time points (two hours and six hours) were also studied with similar results (data not shown). Thus, we concluded that in both the aortic ring assay and in cultures of MLEC cells, IL-6 has direct effects on endothelial cells.

Pericyte coverage is defective in IL-6 stimulated vessels

Over the 7-10 days mouse aortic ring assay incubation period, and the 4 days of the rat aortic ring assay, pericytes also develop around the endothelial cells of the vessel sprouts when they are stimulated by VEGF. Using α-SMA as a pericyte marker, we treated mouse aortic rings with VEGF, mouse or human IL-6 and rat aortic rings with rat IL-6, and we

noticed that pericyte coverage was diminished in the IL-6 stimulated cultures. Overall there were less pericytes attached to the tips of the IL-6 stimulated vessels compared to the VEGF cultures and many detached pericytes were observed in the presence of IL-6. (Figure 3A-C). This difference between number of pericytes associated with the sprout tips in VEGF and IL-6 cultures was significant (Figure 3D). Similar results were observed with another pericyte marker NG2 (Supplementary Figure 4).

Differences in VEGF and IL-6 signaling may explain defective pericyte coverage

We hypothesized that differential regulation of Notch family members may be involved in the differences in pericyte coverage between IL-6 and VEGF-treated cultures. High levels of the Notch ligand DLL4 in endothelial cells are associated with vessel maturity and good pericyte coverage [171819]. Another Notch ligand, Jagged1, is associated with increased vessel sprouting and less mature vessels [2021]. We first investigated this hypothesis in MLEC cells. Using western blotting we found that 24 hours of treatment with IL-6 and VEGF differentially regulated the expression of DLL4 and Jagged1. While IL-6 stimulated more Jagged1 than did VEGF, VEGF had a greater effect on DLL4 than on Jagged1 (Figure 4A, Supplementary Figure 5A). We also observed this differential regulation in IL-6 and VEGF-treated aortic ring lysates (Figure 4B, Supplementary Figure 5B). VEGF stimulation of DLL4 leads to increased activation of the HEY transcription factor [20]. VEGF treatment of MLEC cells increased levels of HEY whereas IL-6 had no effect (Figure 4C, Supplementary Figure 5A). As Ang2 is implicated in the detachment of pericytes from blood vessels [22232425262728], we next investigated if IL-6 also induced Ang2. Figure 4D shows that both VEGF and IL-6 induced Ang2 in both MLEC and the aortic ring model, but IL-6 had a stronger effect (Figure 4D, 4E; Supplementary Figure 5A, B). An earlier time point of 6 hours treatment in MLEC with mIL-6 or VEGF gave similar results (Supplementary Figure 5C). This was also observed in HUVEC after treatment with hIL-6 or VEGF (Supplementary Figure 6). Figure 4F is a summary diagram showing mechanism of action of VEGF or IL-6 on endothelial cells. On binding of VEGF to VEGF receptor leads to upregulation of DLL4 resulting in angiogenesis and maturation of vessels. However, IL-6 binds to IL-6 receptors to activate Jagged1 and Ang2 resulting in angiogenesis with defective pericyte coverage.

Relevance of these findings to malignant disease

Our results so far would suggest that anti-IL-6 treatment would increase pericyte coverage of tumor blood vessels. We previously reported that when peritoneal xenografts of IGROV-1 ovarian cancer cells, that constitutively produce IL-6, were treated with anti-human IL-6 antibodies, vessel density was reduced, as was Jagged1 mRNA and protein [7]. We repeated these experiments with the anti-human IL-6 neutralizing antibody MEDI5117, this time assessing pericyte coverage of the vessels. Using α-SMA (Figure 5A) and NG2 (Figure 5B) as pericyte markers, we found that anti-IL-6 treatment increased pericyte coverage. The sections were scored blind for the level of pericyte coverage of the tumor blood vessels and the effect of anti-IL-6 was statistically significant (Figure 5C). (Supplementary Figure 7A shows an example of the way pericyte coverage was scored).

In addition, immunohistochemistry, IHC, of the anti-IL-6 treated tumors showed decreased Jagged 1 and Ang2 staining and increased DLL4 protein (Figure 5D). The IHC results were scored blind and the results are shown in Supplementary Figure 7B. This was confirmed in western blots of tumor lysates (Figure 5E, Supplementary Figure 7C).

Correlations from human ovarian cancer biopsies

Finally, we revisited a previously published analysis of mRNAs that are associated with high IL-6 expression [7] using publically available datasets of ovarian cancer. Ang2 and Jagged1 had significant a co-efficient of correlation with high IL-6 expression (p=0.015 and p=0.001 respectively) (Figure 6A). Further in-depth analysis of these associations was carried out on RNAseq data from 27 samples of omental metastases from patients with Stage 3/4 high-grade serous ovarian cancer, HGSC. The samples were divided into three groups based on histological analysis; uninvolved omental tissue, established tumor, and stroma with low tumor burden post chemotherapy. Figure 6B shows typical histology of each group. Only within the established tumour groups was a strong and significant correlation (Spearman r) seen between IL-6, Jagged 1 and Ang2 mRNA (Figure 6C). There was no significant correlation between IL-6 and DLL4 mRNA in the same samples (data not shown).

Discussion

A role for IL-6 in pathogenic angiogenesis has been suggested in diseases such as stroke, rheumatoid arthritis and various cancers [29130]. In a previous publication we showed that treatment of ovarian cancer xenografts with an anti-IL-6 antibody reduced the tumor vasculature with concomitant inhibition of the NOTCH ligand Jagged1, which has been implicated in vessel sprouting [7]. Collectively, the published literature suggested that IL-6 could drive abnormal angiogenesis and that the anti-IL-6 antibody had a potential as anti-angiogenic agent. Thus we investigated the direct effects of IL-6 on normal angiogenesis using endothelial *in vitro* and *ex vivo* studies, and used the findings from those studies to explore its importance in tumor angiogenesis using peritoneal models of ovarian cancer and ovarian cancer biopsies.

We found that IL-6 is as potent as VEGF in inducing vessel sprouting in the aortic ring assay and was also able to stimulate endothelial cell migration and proliferation in MLEC cells. VEGFR inhibition studies in the aortic ring model and protein analysis of downstream VEGF and IL-6 signaling indicate that the angiogenic effects observed with IL-6 may not depend on VEGF in endothelial cells. The effects on IL-6 on malignant cells may be different because of the complex autocrine signaling networks generated in cancer cells. Preliminary experiments on malignant cell lines showed that, in contrast to endothelial cells, IL-6 can stimulate VEGF signaling and *vice versa*. Additionally, in the RNAseq experiments of Figure 6, we found that there was a positive association between IL-6 and VEGF mRNA levels, but this would be expected when studying isolates from a complex multi-cellular tumor microenvironment. Hence we suspect that IL-6 may have different effects on malignant cells and endothelial cells.

We found that the angiogenesis stimulated by IL-6 leads to formation of vasculature with defective pericyte coverage, and that anti-IL-6 treatment of the peritoneal ovarian cancer xenografts leads to restoration of pericytes on the blood vessels. Investigating the mechanism of action of IL-6 and VEGF in inducing this different phenotype of vessel maturation has shown roles for Notch ligands and Ang2.

This is, to our knowledge, the first study showing that IL-6 can induce a type of vessel sprouting with abnormal pericyte coverage compared to VEGF. These observations have clinical implications for malignant and other diseases, especially as studies in various cancers suggest that pericyte depletion leads to increased metastasis [223132]. The ability of anti-IL-6 treatment to improve pericyte coverage of vessels in xenograft models suggests that in the tumor microenvironment, defective pericyte coverage may be due to the action of IL-6 in those tumors with high levels of this cytokine.

The regulation of Ang2 by IL-6 is another interesting finding as Ang2 expression has been shown to correlate with lymph node metastasis in various cancers [33, 34, 35]. Moreover, the angiopoietin inhibitor Trebananib increased progression-free survival in patients with recurrent ovarian cancer [36].

As STAT3 signaling is implicated in the treatment failure of various anti-angiogenic agents [13373839], combinations of IL-6 and angiogenesis antagonists may be worthy of further study.

Supplementary Material

Refer to Web version on PubMed Central for supplementary material.

Acknowledgments

Frances Balkwill acknowledges support from Cancer Research UK Programme Grant C587/A16354, European Research Council Advanced Grant no 322566

James R. Whiteford acknowledges support from Arthritis Research-UK Grant no 19207

References

1. Taniguchi K, Karin M. IL-6 and related cytokines as the critical lynchpins between inflammation and cancer. Seminars in immunology. 2014; 26:54–74. [PubMed: 24552665]
2. Hong DS, Angelo LS, Kurzrock R. Interleukin-6 and its receptor in cancer: implications for translational therapeutics. Cancer. 2007; 110:1911–1928. [PubMed: 17849470]
3. Ancrile B, Lim KH, Counter CM. Oncogenic Ras-induced secretion of IL6 is required for tumorigenesis. Genes Dev. 2007; 21:1714–1719. [PubMed: 17639077]
4. Grivennikov S, et al. IL-6 and Stat3 Are Required for Survival of Intestinal Epithelial Cells and Development of Colitis-Associated Cancer. Cancer Cell. 2009; 15:103–113. [PubMed: 19185845]
5. Chang Q, et al. The IL-6/JAK/Stat3 feed-forward loop drives tumorigenesis and metastasis. Neoplasia. 2013; 15:848–862. [PubMed: 23814496]
6. Kulbe H, et al. A Dynamic Inflammatory Cytokine Network in the Human Ovarian Cancer Microenvironment. Cancer research. 2012; 72:66–75. [PubMed: 22065722]
7. Coward J, et al. Interleukin-6 as a Therapeutic Target in Human Ovarian Cancer. Clinical cancer research: an official journal of the American Association for Cancer Research. 2011; 17:6083–6096. [PubMed: 21795409]

8. Stone RL, et al. Paraneoplastic thrombocytosis in ovarian cancer. The New England journal of medicine. 2012; 366:610–618. [PubMed: 22335738]
9. Nilsson MB, Langley RR, Fidler IJ. Interleukin-6, secreted by human ovarian carcinoma cells, is a potent proangiogenic cytokine. Cancer Res. 2005; 65:10794–10800. [PubMed: 16322225]
10. Xu Q, et al. Targeting Stat3 blocks both HIF-1 and VEGF expression induced by multiple oncogenic growth signaling pathways. Oncogene. 2005; 24:5552–5560. [PubMed: 16007214]
11. Yao JS, Zhai W, Young WL, Yang GY. Interleukin-6 triggers human cerebral endothelial cells proliferation and migration: the role for KDR and MMP-9. Biochem Biophys Res Commun. 2006; 342:1396–1404. [PubMed: 16516857]
12. Fan Y, et al. Interleukin-6 stimulates circulating blood-derived endothelial progenitor cell angiogenesis in vitro. Journal of cerebral blood flow and metabolism: official journal of the International Society of Cerebral Blood Flow and Metabolism. 2008; 28:90–98.
13. de Groot J, et al. Modulating antiangiogenic resistance by inhibiting the signal transducer and activator of transcription 3 pathway in glioblastoma. Oncotarget. 2012; 3:1036–1048. [PubMed: 23013619]
14. Kwon KA, et al. Clinical significance of preoperative serum vascular endothelial growth factor, interleukin-6, and C-reactive protein level in colorectal cancer. BMC Cancer. 2010; 10:203. [PubMed: 20465852]
15. Cohen T, Nahari D, Cerem LW, Neufeld G, Levi BZ. Interleukin 6 induces the expression of vascular endothelial growth factor. J Biol Chem. 1996; 271:736–741. [PubMed: 8557680]
16. Reynolds LE, Hodivala-Dilke KM. Primary mouse endothelial cell culture for assays of angiogenesis. Methods in molecular medicine. 2006; 120:503–509. [PubMed: 16491622]
17. Patel NS, et al. Up-regulation of endothelial delta-like 4 expression correlates with vessel maturation in bladder cancer. Clin Cancer Res. 2006; 12:4836–4844. [PubMed: 16914569]
18. Scehnet JS, et al. Inhibition of Dll4-mediated signaling induces proliferation of immature vessels and results in poor tissue perfusion. Blood. 2007; 109:4753–4760. [PubMed: 17311993]
19. Schadler KL, Zweidler-McKay PA, Guan H, Kleinerman ES. Delta-like ligand 4 plays a critical role in pericyte/vascular smooth muscle cell formation during vasculogenesis and tumor vessel expansion in Ewing's sarcoma. Clin Cancer Res. 2010; 16:848–856. [PubMed: 20103680]
20. Benedito R, et al. The notch ligands Dll4 and Jagged1 have opposing effects on angiogenesis. Cell. 2009; 137:1124–1135. [PubMed: 19524514]
21. Kume T. Novel insights into the differential functions of Notch ligands in vascular formation. Journal of angiogenesis research. 2009; 1:8. [PubMed: 20016694]
22. Gerhardt H, Semb H. Pericytes: gatekeepers in tumour cell metastasis? Journal of molecular medicine. 2008; 86:135–144. [PubMed: 17891366]
23. Qin D, et al. Early vessel destabilization mediated by Angiopoietin-2 and subsequent vessel maturation via Angiopoietin-1 induce functional neovasculature after ischemia. PLoS One. 2013; 8:e61831. [PubMed: 23613948]
24. Feng Y, et al. Impaired pericyte recruitment and abnormal retinal angiogenesis as a result of angiopoietin-2 overexpression. Thrombosis and haemostasis. 2007; 97:99–108. [PubMed: 17200776]
25. Hammes HP, et al. Angiopoietin-2 causes pericyte dropout in the normal retina: evidence for involvement in diabetic retinopathy. Diabetes. 2004; 53:1104–1110. [PubMed: 15047628]
26. Keskin D, et al. Targeting Vascular Pericytes in Hypoxic Tumors Increases Lung Metastasis via Angiopoietin-2. Cell reports. 2015; 10:1066–1081. [PubMed: 25704811]
27. Ribatti D, Nico B, Crivellato E. The role of pericytes in angiogenesis. Int J Dev Biol. 2011; 55:261–268. [PubMed: 21710434]
28. Armulik A, Abramsson A, Betsholtz C. Endothelial/pericyte interactions. Circulation research. 2005; 97:512–523. [PubMed: 16166562]
29. Gertz K, et al. Essential role of interleukin-6 in post-stroke angiogenesis. Brain: a journal of neurology. 2012; 135:1964–1980. [PubMed: 22492561]
30. Kayakabe K, et al. Interleukin-6 promotes destabilized angiogenesis by modulating angiopoietin expression in rheumatoid arthritis. Rheumatology. 2012; 51:1571–1579. [PubMed: 22596210]

31. Xian X, et al. Pericytes limit tumor cell metastasis. J Clin Invest. 2006; 116:642–651. [PubMed: 16470244]
32. Cooke VG, et al. Pericyte depletion results in hypoxia-associated epithelial-to-mesenchymal transition and metastasis mediated by met signaling pathway. Cancer cell. 2012; 21:66–81. [PubMed: 22264789]
33. Jo MJ, et al. Preoperative serum angiopoietin-2 levels correlate with lymph node status in patients with early gastric cancer. Annals of surgical oncology. 2009; 16:2052–2057. [PubMed: 19408052]
34. Sfiligoi C, et al. Angiopoietin-2 expression in breast cancer correlates with lymph node invasion and short survival. Int J Cancer. 2003; 103:466–474. [PubMed: 12478661]
35. Schulz P, et al. Angiopoietin-2 drives lymphatic metastasis of pancreatic cancer. Faseb J. 2011; 25:3325–3335. [PubMed: 21685330]
36. Monk BJ, et al. Anti-angiopoietin therapy with trebananib for recurrent ovarian cancer (TRINOVA-1): a randomised, multicentre, double-blind, placebo-controlled phase 3 trial. Lancet Oncol. 2014; 15:799–808. [PubMed: 24950985]
37. Jain RK, et al. Biomarkers of response and resistance to antiangiogenic therapy. Nat Rev Clin Oncol. 2009; 6:327–338. [PubMed: 19483739]
38. Willett CG, et al. Efficacy, safety, and biomarkers of neoadjuvant bevacizumab, radiation therapy, and fluorouracil in rectal cancer: a multidisciplinary phase II study. J Clin Oncol. 2009; 27:3020–3026. [PubMed: 19470921]
39. Zhu AX, et al. Efficacy, safety, and potential biomarkers of sunitinib monotherapy in advanced hepatocellular carcinoma: a phase II study. J Clin Oncol. 2009; 27:3027–3035. [PubMed: 19470923]
40. Nicosia RF. The aortic ring model of angiogenesis: a quarter century of search and discovery. Journal of cellular and molecular medicine. 2009; 13:4113–4136. [PubMed: 19725916]

Europe PMC Funders Author Manuscripts

Europe PMC Funders Author Manuscripts

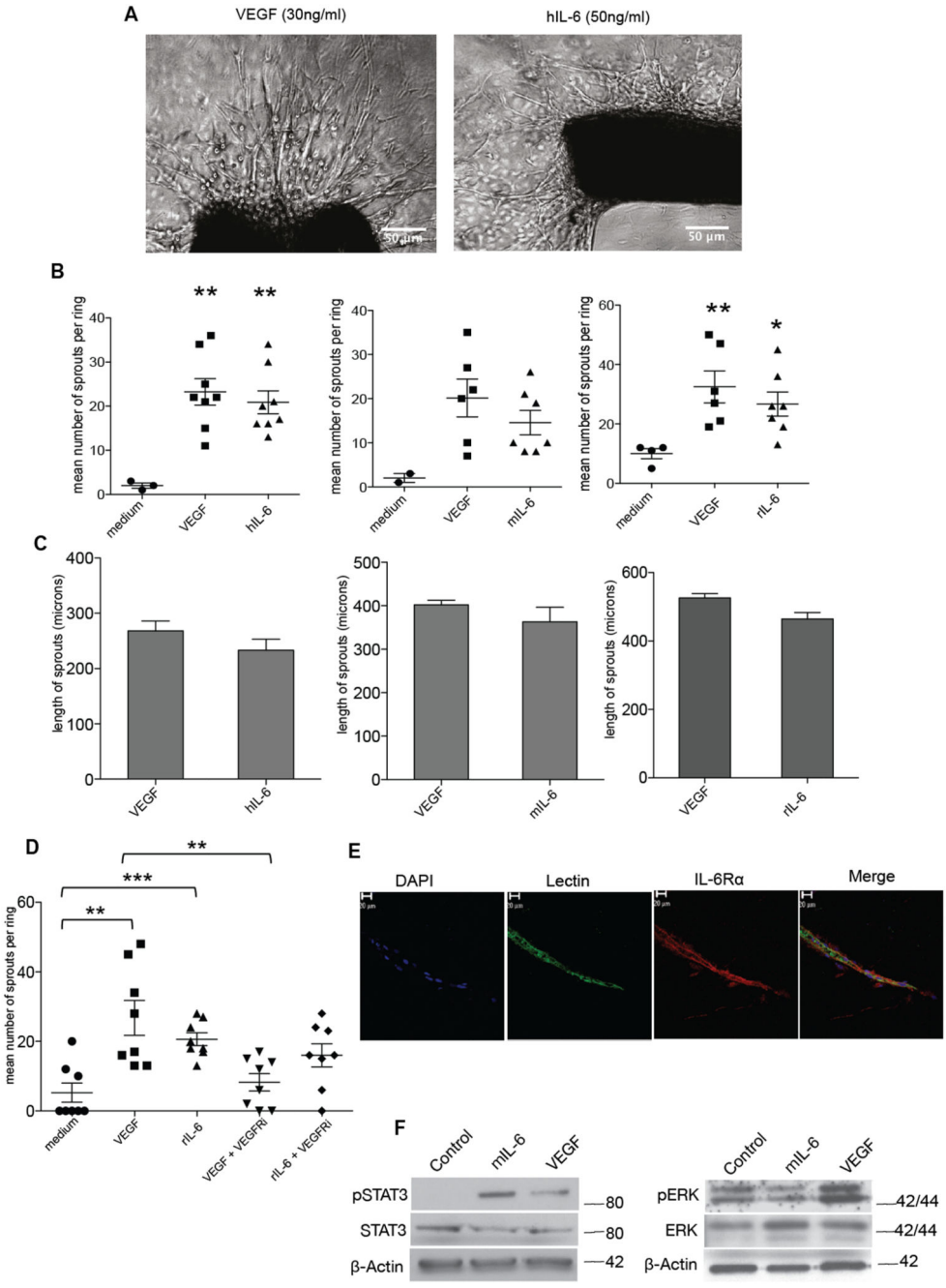

Figure 1. IL-6 stimulates angiogenesis in the aortic ring assay

A. Phase contrast images of aortic rings embedded in collagen I with the indicated concentrations of VEGF or human IL-6. Human and mouse IL-6 experiments were carried out with aortas isolated from wild-type C57BL/6 mice (8–12 weeks) and rat IL-6 experiments were carried out with aortas isolated from Wistar rats weighing 180-200g. **B.** Angiogenic sprouts were counted after a week in culture for mouse aortic rings or after 4 days in culture for the rat aortic rings following treatment with VEGF, hIL-6 or mIL-6 or rIL-6. Significant increases in microvessel sprouting are observed in VEGF and IL-6 treated

rings (n=9 per group) compared with PBS-treated controls, however no difference in number of sprouts is observed between VEGF and IL-6 treated rings. The p value for medium vs VEGF ($p<0.058$) and medium vs VEGF (0.054) just failed to reach significance. Statistical analysis carried out using student T-test is shown as (**) $p \leq 0.01$; (***) $p \leq 0.001$. **C.** Length of sprouts was measured using ImageJ analysis. Mean length of sprouts (n=9 per group) shows no significant difference between the VEGF and IL-6 treated sprouts. **D.** 10nM of VEGFRi inhibited vessel sprouting in VEGF (10ng/ml) treated rings but not in rat IL-6 (10ng/ml) treated rings. Statistical analysis carried out using student T-test is shown as (**) $p \leq 0.01$; (***) $p \leq 0.001$ **E.** Aortic ring vessel stained for endothelial cells using BS1 lectin (green) and for IL-6Rα (red). **F.** Western blot analysis of protein extracted from mouse aortas treated with VEGF (30ng/ml) or mouse IL-6 (30ng/ml). Mouse IL-6 activated downstream pSTAT3 and VEGF induced downstream pERK levels.

Europe PMC Funders Author Manuscripts

Europe PMC Funders Author Manuscripts

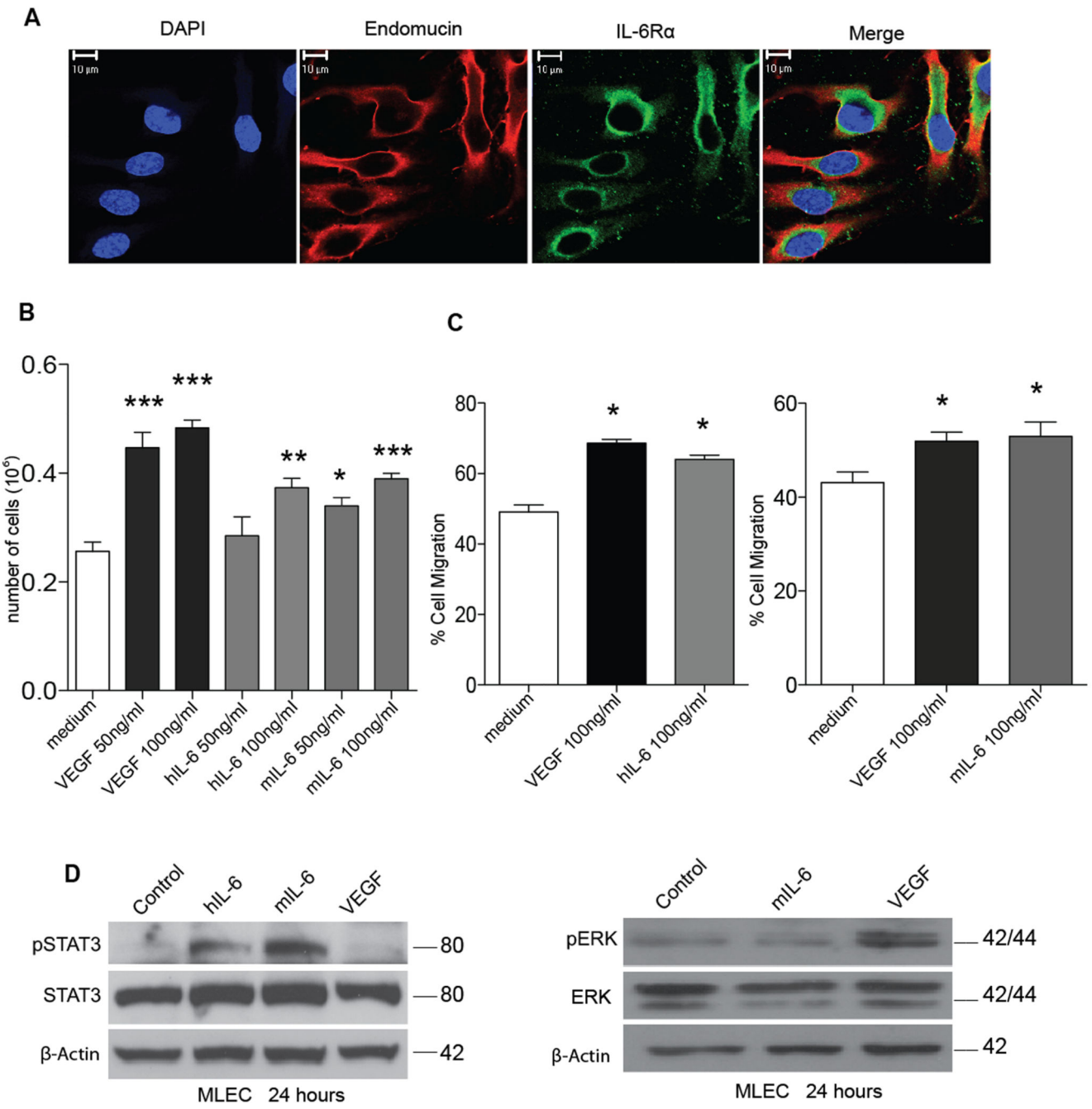

Figure 2. IL-6 has direct effects on mouse lung endothelial cells

A. Immunocytochemistry staining for endomucin (red) and IL-6Rα (green) on MLEC. **B.** 70,000 MLEC were plated and treated with either PBS (control) and indicated concentrations of VEGF or IL-6 for 72 hours. The cells were then trypsinized and counted using a cell counter and the mean of the triplicates were calculated. Proliferation assay shows a significant increase in proliferation with VEGF (50 or 100ng/ml), human IL-6 (100ng/ml) and mouse IL-6 (50 or 100ng/ml). **C.** Scratch assay using a time-lapse microscope was used to measure the migration of MLEC after treatment with VEGF and

IL-6. Significant increases in cell migration are observed with VEGF or IL-6 treated MLEC after 16 hours. Statistical analysis carried out using student T-test is shown as (*) $p \leq 0.05$: (**) $p \leq 0.01$; (***) $p \leq 0.001$ **D.** Western blot analysis of protein extracted from MLEC treated with IL-6 (30ng/ml) or VEGF (30ng/ml) for 24 hours. IL-6 induced downstream pSTAT3 and VEGF induced downstream pERK levels, indicating both pathways are independent of each other for signaling in MLEC.

Europe PMC Funders Author Manuscripts

Europe PMC Funders Author Manuscripts

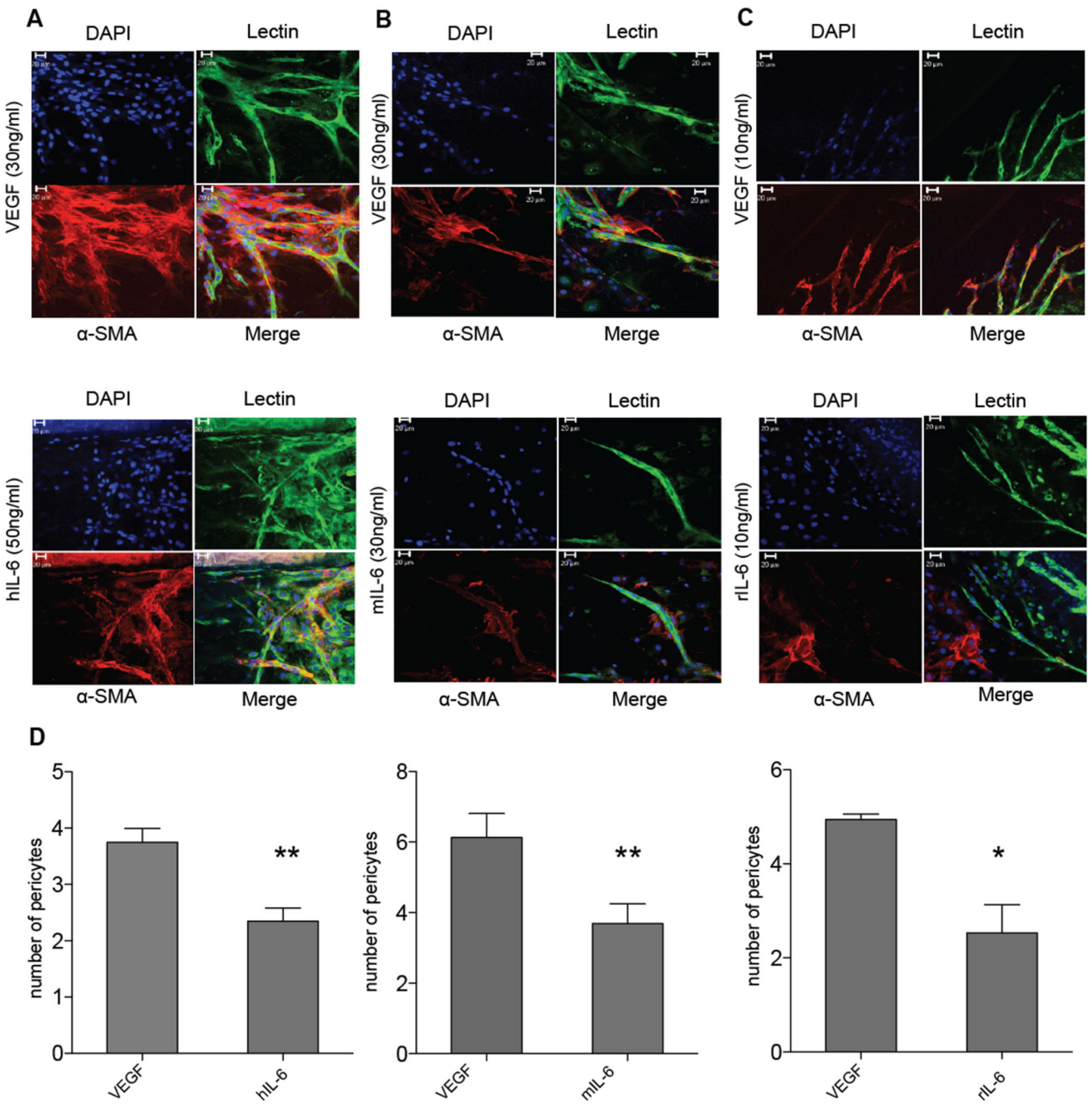

Figure 3. Pericyte coverage is defective in IL-6 stimulated vessels

Aortic rings grown in type I collagen were stained for endothelial cells using BS1 lectin (green) and antibodies to α-SMA (red) after treatment with VEGF (top panels) or (**A**) human IL-6, **(B)** mouse IL-6 or (**C**) rat IL-6 (bottom panels). Confocal microscopy taken using a Zeiss LSM 510 laser-scanning microscope (×40) show VEGF treated vessels with good pericyte coverage and IL-6 treated vessels with poor pericyte coverage. **D.** Significant difference is observed in pericyte coverage between the VEGF and IL-6 treated vessels.

Statistical analysis carried out using student t-test is shown as (*) $p \leq 0.05$: (**) $p \leq 0.01$; (***) $p \leq 0.001$ (n=5-9 aortas per condition).

Europe PMC Funders Author Manuscripts

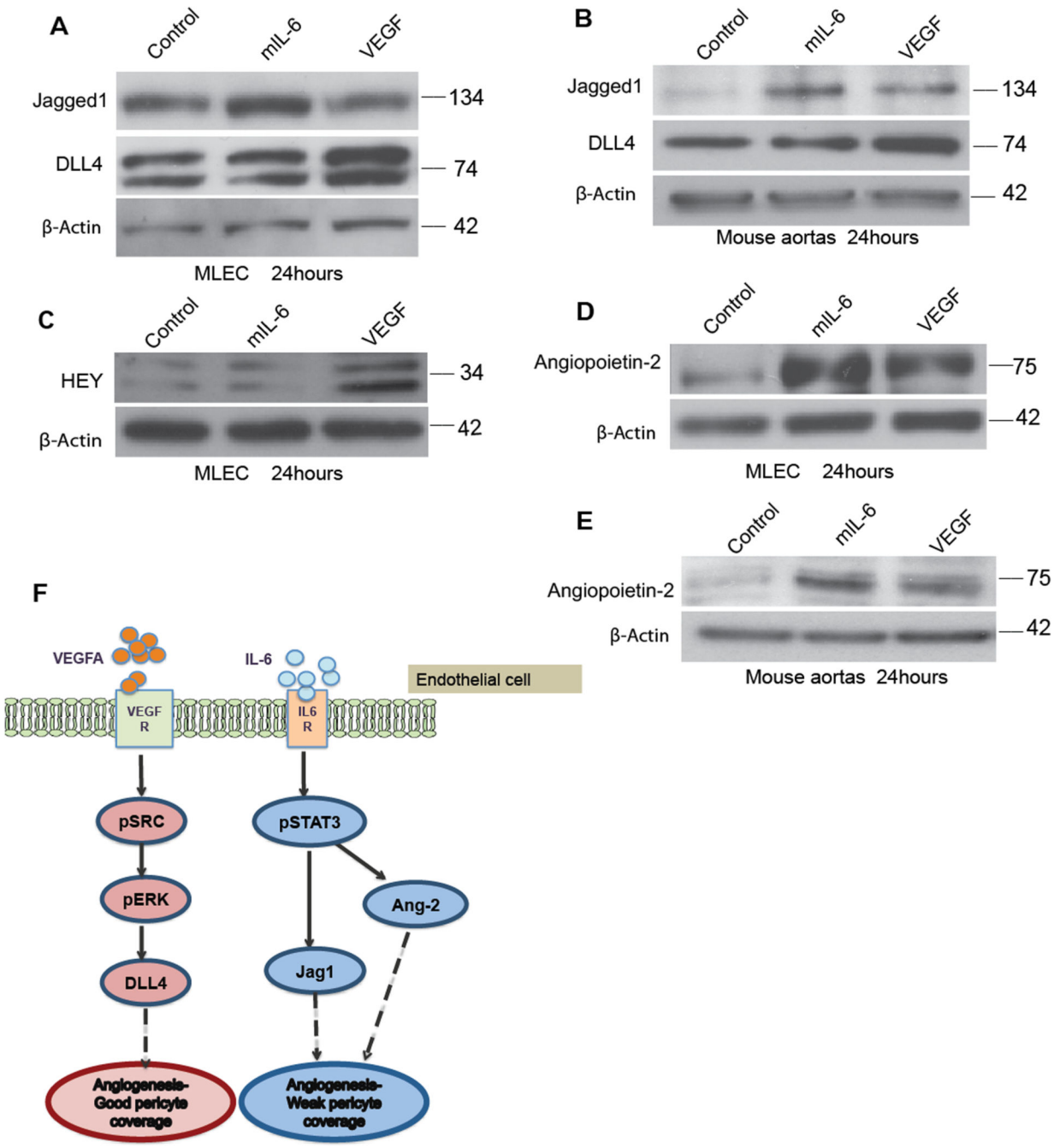

Figure 4. Differential regulation of VEGF and IL-6 mediated Notch ligands and Ang2 may explain defective pericyte coverage

2×10^5 MLEC cells were plated and treated with control (PBS), VEGF (30ng/ml) or mIL-6 (30ng/ml) for 24 hours. **A.** Western blot analysis of Jagged1 and DLL4 expression on MLEC cells. **B.** The induction of Jagged1 by IL-6 and DLL4 by VEGF is further confirmed in the protein analysis of aortas treated with IL-6 or VEGF. **C.** Hey upregulation in the VEGF treated MLEC confirms the positive VEGF induced Notch-DLL4 interaction in the MLEC. **D.** Western blot analysis of Ang2 in the MLEC treated with VEGF or IL-6 shows

Europe PMC Funders Author Manuscripts

similar upregulation of Ang2 in the MLEC treated with IL-6 compared to VEGF **E.** Ang2 expression in protein isolated from three aortas per group from wild-type C57BL/6 mice (8–12 weeks) and treated with either VEGF (30ng/ml) or mouse IL-6 (30ng/ml) for 24hours **F.** Model for mechanism of action of VEGF or IL-6 on endothelial cells. VEGF binding to VEGF receptor leads to upregulation of DLL4 resulting in angiogenesis and maturation of vessels. However, IL-6 forms a complex with IL-6 receptors to activate Jagged1 and Ang2 resulting in angiogenesis with weak or defective pericyte coverage.

Europe PMC Funders Author Manuscripts

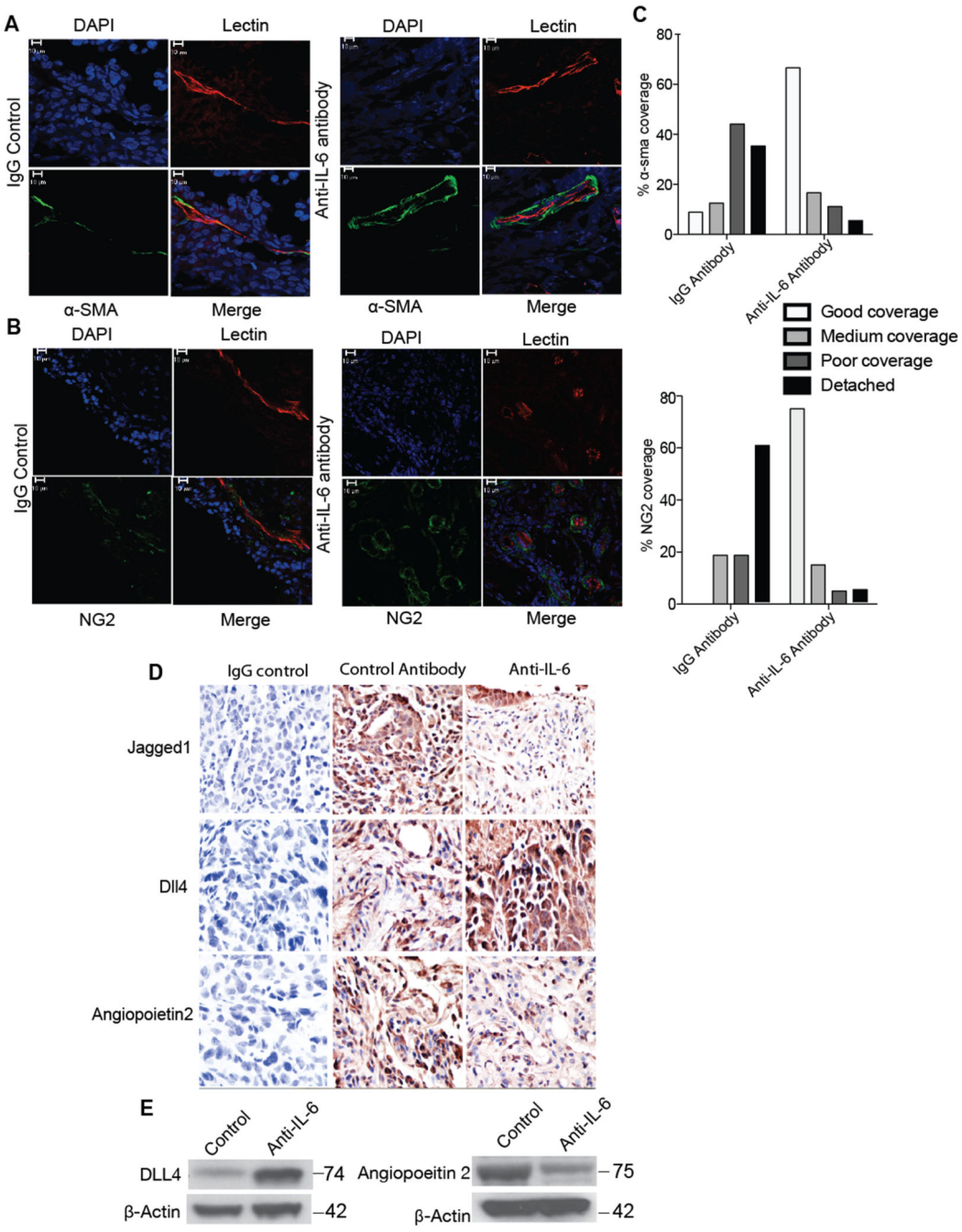

Figure 5. Effects of anti-IL-6 antibody on *in vivo* IGROV-1 vasculature

1×10^7 IGROV-1-luc cells were injected i.p. into 8 weeks old Balb/c nude female mice. After 24 hours the mice were treated with either control IgG antibody (20mg/kg) or anti-IL-6 antibody (20mg/kg) twice a week for 4 weeks. Following this, three of the animals from each group were injected with TRITC-conjugated *Bandeiraea* via the tail vein, 3 min before being perfused with 4% paraformaldehyde. The lectin stained frozen sections were stained for α-SMA (green) (**A**) or NG2 (green) (**B**). Treatment with anti-IL-6 antibody was able to restore the pericyte coverage in IGROV-1 xenografts. Staining of α-SMA and NG2 staining

show poor or detached pericyte coverage in the IgG antibody group compared to good pericyte coverage in the anti-IL-6 treated group. **C.** Quantification of the staining show a significant difference between the IGROV-1 antibody control and anti-IL-6 treated group (p value < 0.001). The quantification carried out by two independent reviewers was analyzed using chi-sqaure test (n=6 per group from two independent experiments). **D**. Immunohistochemistry staining for Jagged1, DLL4 and Ang2 in the IGROV-1 xenograft following 4 weeks of treatment with anti-IL-6 antibody. The images were taken from 5 randomly selected areas per tumor section (n=6 per group from two independent experiments) using a ×40 microscope. **E.** Western blot analysis of DLL4 and Ang2 from protein extracted from *in vivo* IGROV-1 xenografts treated with anti-IL-6 antibody.

Europe PMC Funders Author Manuscripts

A

Gene symbol	Gene description	P value
ANGPT2	Angiopoietin2	0.015
JAG1	Jagged1	0.001

B

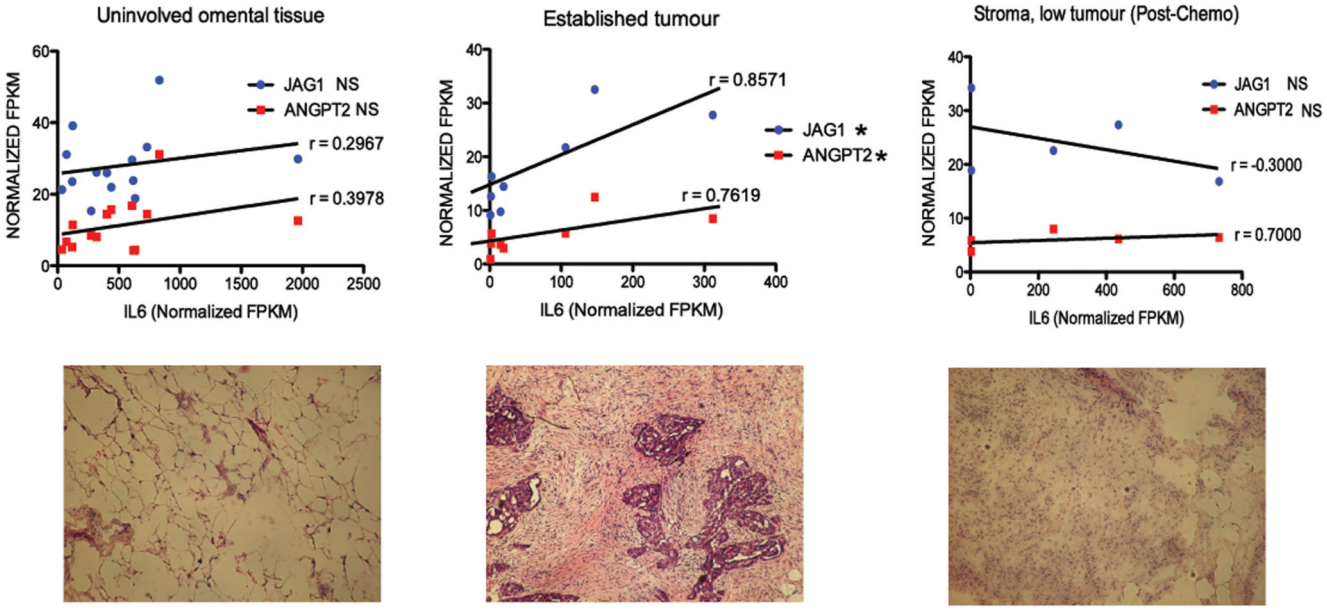

Figure 6. Relevance of these findings to malignant disease

Gene expression data from 285 ovarian cancer biopsies from the AOCS (Australian Ovarian Cancer Study) dataset along with 245 samples obtained by merging two other publicly available datasets were ranked for expression of IL-6 pathway genes. Then 50 samples with the highest (high IL-6) and 50 samples with the lowest (low IL-6) levels of expression were selected and from that a list was generated of the differentially expressed genes between the high and low IL-6 samples. These differentially expressed genes were then associated with various pathways and processes. Significant associations were found between the high IL-6 pathway gene expression and with various processes including angiogenesis. **A.** The high IL-6 pathway expression correlated positively with Jagged1 and Ang2. RNAseq analysis of omental metastases from patients with stage 3-4 high-grade serous ovarian cancer. The 27 tumor samples were divided into three groups based on histological analysis; uninvolved omental tissue, established tumors and stroma with low tumor burden post chemotherapy. **B.** Significant positive correlation was observed between expression levels for IL-6, Jagged 1 and Ang2 mRNA, and the best-fit correlation (Spearman r) was found in samples that had a high burden of tumor.